The nanoscopic structure of annealed $Ge_{20}Te_{80}$ glass: quasi-atomic-scale imaging using atomic-force microscopy

1995 J. Phys.: Condens. Matter 7 L135

(http://iopscience.iop.org/0953-8984/7/10/003)

J. Phys.: Condens. Matter 7 (1995) L135–L139. Printed in the UK

LETTER TO THE EDITOR

The nanoscopic structure of annealed $Ge_{20}Te_{80}$ glass: quasi-atomic-scale imaging using atomic-force microscopy

Kazuhiko Ichikawa

Division of Material Science, Graduate School of Environmental Earth Science, Hokkaido University, Sapporo 060, Japan

Received 19 January 1995

Abstract. The nanoscopic structure of annealed $Ge_{20}Te_{80}$ glasses has been observed using atomic-force microscopy (AFM). The AFM images reveal to some extent the structure of amorphous semiconductors. AFM images as large as 20×20–50×50 nm^2 have shown many particles with diameters 2.5–3.5 nm—of the same order of magnitude as the interparticle distance. Since the peaks for each alignment lie at roughly the same height, it has been possible to image a couple of linear alignments 15–20 nm in length by AFM. The two-dimensional alignments generated a pseudo-surface (or infant surface) around 15×10 nm^2 in area. With the aid of our previous work on the quasi-atomic-scale images observed by scanning tunnelling microscopy and on the diffraction data from neutron scattering, the nanoscopic structure of annealed $Ge_{20}Te_{80}$ glasses can be interpreted in terms of short-range order (SRO), medium-range order (MRO) and supramedium-range order (SMRO) (the regions are $\simeq$0.5 nm, $\simeq$2.5–3.5 nm and $\simeq$15–20 nm, respectively). The SMRO should be established by pseudo-ordered alignment or rings of the particles characterized by MRO of diameter 2.5–3.5 nm; the MRO should be established by pseudo-ordered arrangements among the structural units characterized by SRO.

What is the origin of structural relaxation? We want to see some direct experimental evidence to indicate whether the structural relaxation well below the glass transition temperature T_g is attributable to collective reorientation among the structural units or to the changes in the atomic distances and the bond angles in the structural units. The structure of the glasses (Elliott 1991, Suzuki 1987) can be interpreted in terms of (i) chemical short-range order (CSRO or SRO) which characterizes the structural units by using the nearest-neighbour distance, the coordination number $n_{\alpha\beta}$ of the β-atoms around an α-atom, and the bond angle (or the second-nearest-neighbour distance) and (ii) medium-range order (MRO) which appears in the geometrical conformations among the units.

The effect of annealing on the SRO and MRO cannot be observed via the neutron diffraction measurements for the $Ge_{20}Te_{80}$ glass annealed for ten days below T_g: (i) the change in the positions of the first and second peaks (i.e. the nearest- and second-neighbour distances) cannot be observed within the experimental limit of length changes of 0.01 Å (Ichikawa *et al* 1987); (ii) the first small and sharp diffraction peak (FSDP) of the structure factor has never shown the effect of low-temperature annealing (Ichikawa *et al* 1987). The FSDP is the manifestation of MRO in covalent glasses and liquids. Many theoretical and experimental studies have been performed on the premise that the FSDP originates from correlations among the cation-centred structural units/clusters of the layers or the alignments. It has also been proposed that the FSDP arises from the presence of zones of low atomic occupancy (Fowler and Elliott 1987). The low-density regions themselves can then serve to define the spatial extent of MRO among the units. In conclusion, no structural relaxation

0953-8984/95/100135+05$19.50

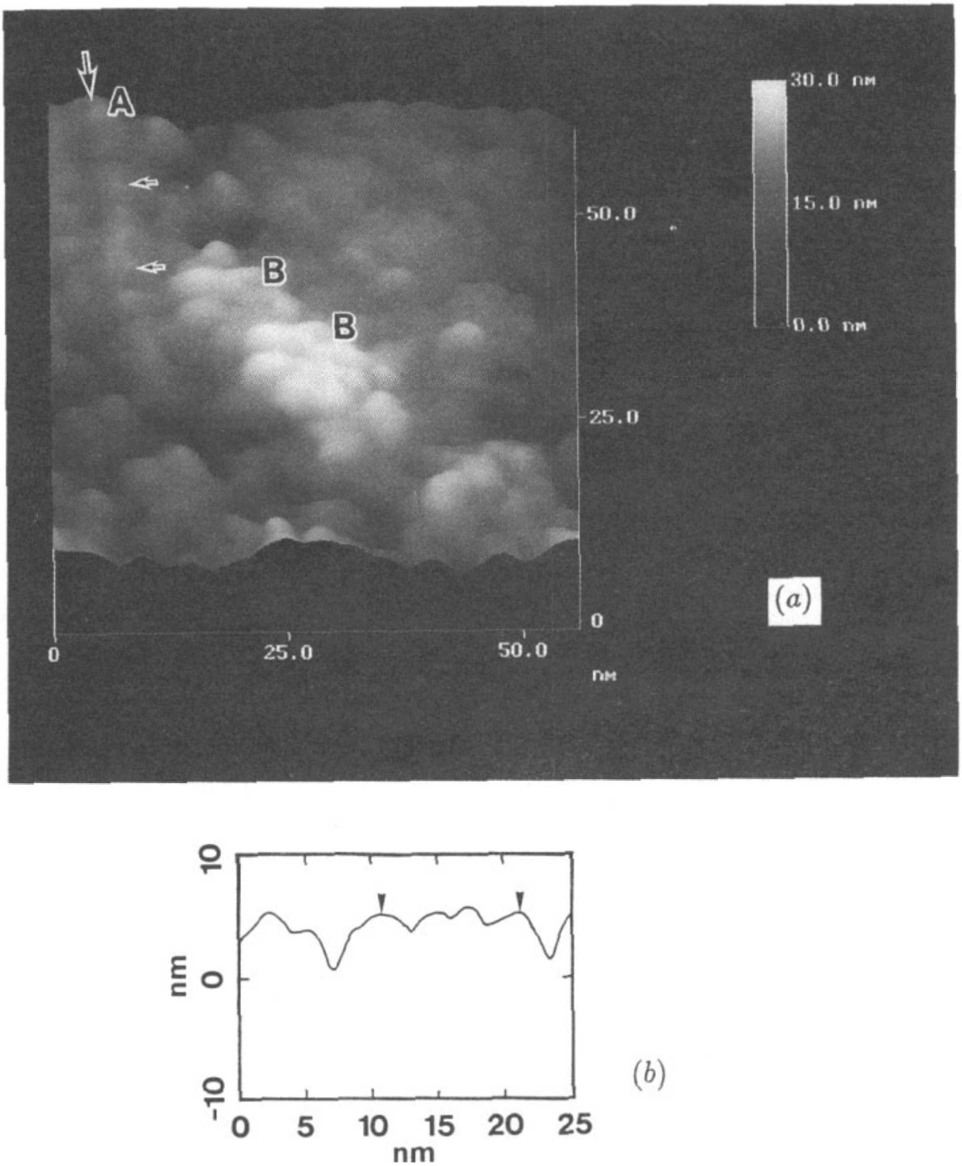

Figure 1. (*a*) A 50 × 50 nm^2 AFM image of annealed $Ge_{20}Te_{80}$ glass. B is described in the text. (*b*) An interpolated cross-section profile taken from the alignment along the axis A in (*a*). The distance between the two arrows is ≃10 nm.

process gave rise to pronounced changes in the dimension of MRO for the $Ge_{20}Te_{80}$ glass because there was no change in the FSDP under low-temperature annealing (Ichikawa *et al* 1987).

It has, however, become clear—on the basis of data on the heat capacity C_p of the $Ge_{20}Te_{80}$ glasses—that the low-temperature ($<T_g$) relaxation is governed by the kinetics associated with exothermic reaction and the decrease of reversible entropy during annealing (Xu and Ichikawa 1986). The effect of annealing on the structure of $Ge_{20}Te_{80}$ glass has been further examined in quasi-atomic-scale images obtained by using scanning tunnelling

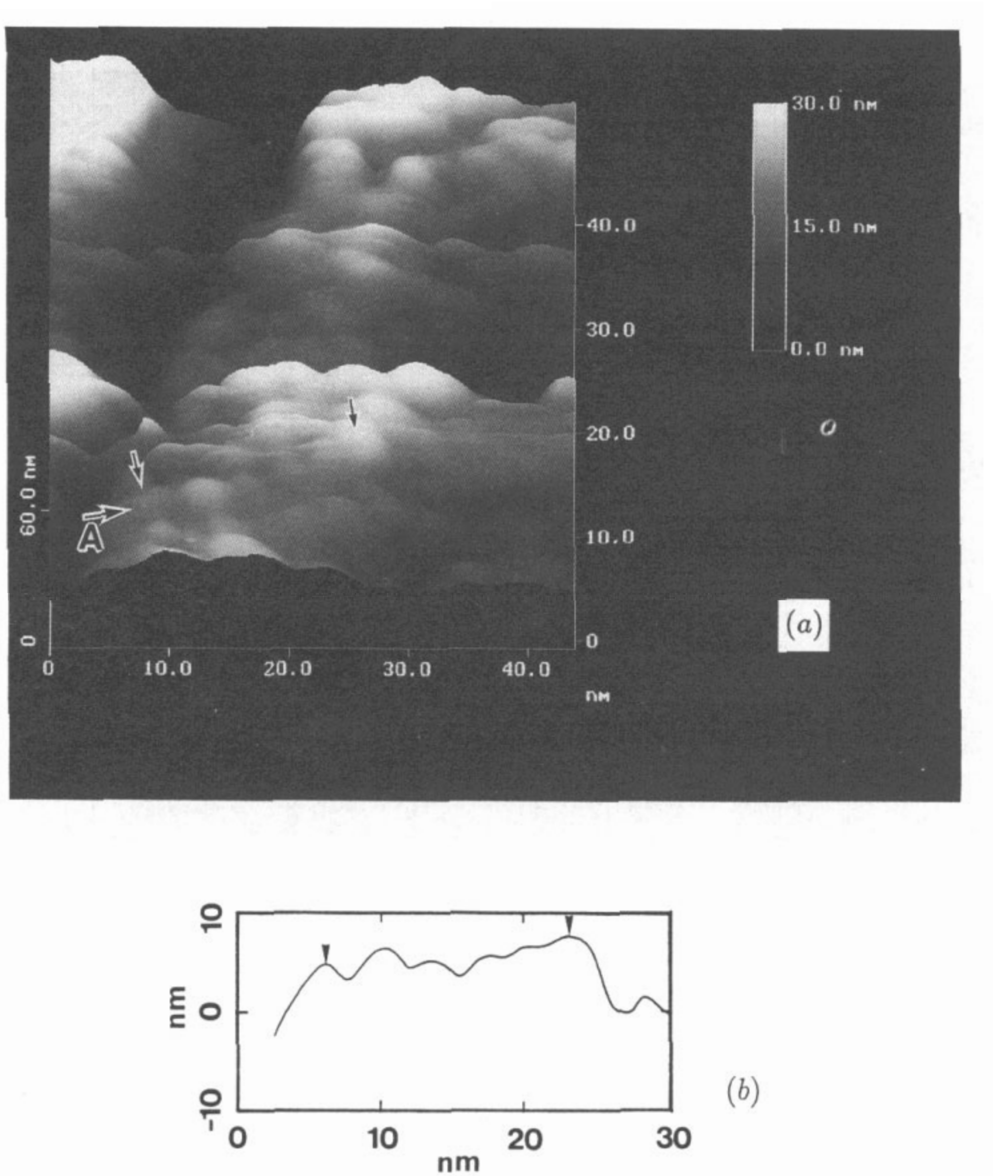

Figure 2. (*a*) A 40 × 40 nm^2 AFM image of annealed $Ge_{20}Te_{80}$ glass. B is described in the text. (*b*) An interpolated cross-section profile taken from the alignment along the axis A in (*a*). The distance between the two arrows is 17 nm.

microscopy (STM) (Ichikawa 1992). STM images as large as $\simeq$100 nm^2 have provided quasi-atomic-resolution ridges $\simeq$3 nm in length. The nearest-neighbour distance between peaks in each alignment is $\simeq$0.5 nm; alignments in parallel are separated by $\simeq$0.7 nm. These ridges can generate the surface associated with pseudo-flatness; its area is $\lesssim$10 nm^2.

In this work we report on images, observed by atomic-force microscopy (AFM), of the alignments or rings consisting of particles that are characteristic of MRO for annealed $Ge_{20}Te_{80}$ glass and propose supramedium-range order (SMRO), whose extent should be >10 nm.

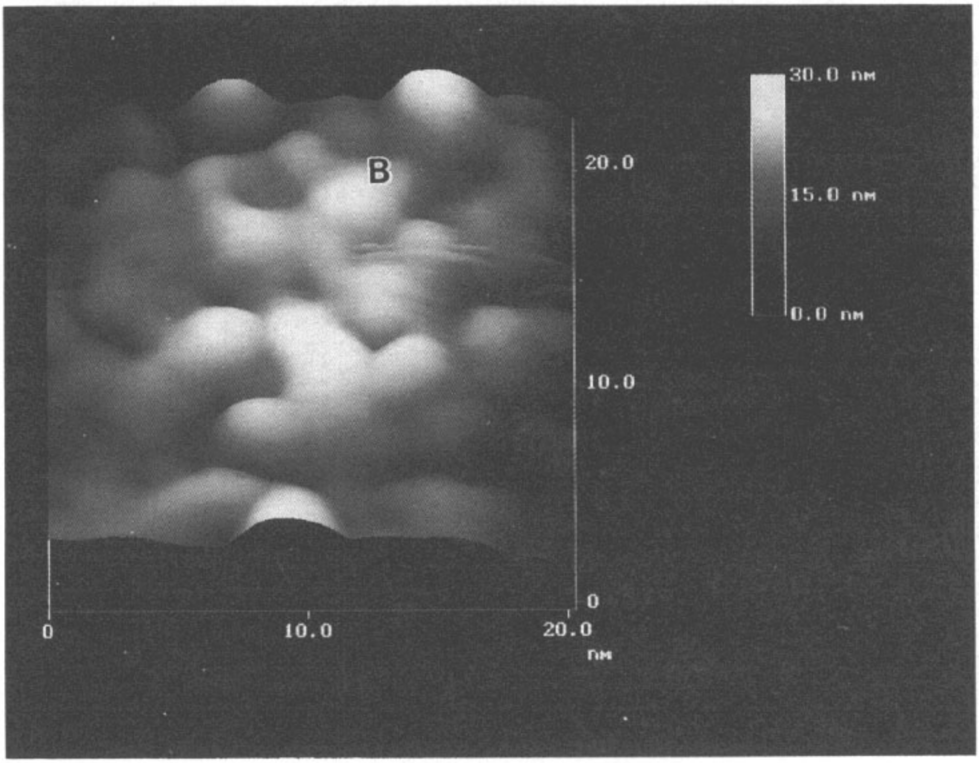

Figure 3. A 20 × 20 nm^2 AFM image of annealed $Ge_{20}Te_{80}$ glass. B is described in the text.

The preparation and examination of $Ge_{20}Te_{80}$ glass have been described in a previous paper (Xu and Ichikawa 1986). The $Ge_{20}Te_{80}$ glass was annealed for three days at 100 °C well below T_g (i.e. 155.5 ± 1.0 °C), which was taken as the point of inflection of the C_p–T-curve.

All the AFM images in the present work were measured in the constant-force mode (Binnig *et al* 1986). The sample surface was imaged, mechanically tracing its topography using a microfabricated cantilever with an integrated pyramidal Si_3N_4 tip. The deflections of the cantilever were caused by surface features and detected via a laser beam reflected off the back of the cantilever into a two-segment photodiode for position sensing. A feedback loop moves the z-translator as necessary to keep the beam position constant or to maintain a constant force between the $Ge_{20}Te_{80}$ glass and the tip. The z-axis displacement is read as the height of the surface features of the glass. In our experiments the scanning force was less than 10 nN, and the image-acquisition time was 20 s.

Images were taken in air for various regions of a piece of $Ge_{20}Te_{80}$ glass plate; much of the surface was too rough to provide valid AFM images. Since non-crystalline solids such as $Ge_{20}Te_{80}$ glass have no cleavage planes identified by sets of Miller indices (hkl), much more extensive searching was undertaken to find a flat plane at least as large as 100 nm^2, which could allow quasi-atomic-scale resolution to be achieved in the AFM images. Atomic-resolution images of highly oriented NaCl(001) surface could be taken in air for many regions of the plate: there were no air/moisture contamination effects (Yamada and

Ichikawa 1994). Air/moisture-effect-free AFM images of freshly crushed $Ge_{20}Te_{80}$ glass may be observed in air after a rinsing in ethanol.

Figure 1 shows a 50×50 nm^2 AFM image; there are many particles 2.5–3.5 nm in diameter and some of them appear to display a linear alignment (marked A) $\simeq$15 nm in length. At the front of the image (marked B) rings generate a pseudo-surface (or infant surface) as large as $\simeq$100 nm^2. 40×40 and 20×20 nm^2 images of another sample are shown in figures 2 and 3 respectively. A couple of linear alignments 15–20 nm in length are observable at the front of the image of figure 2. A small ring $\simeq$10 nm in diameter (marked B) is imaged in figure 3. The peaks for each alignment lie at roughly the same height and at a distance of 3.0–3.5 nm, as shown in the interpolated cross-section profiles, taken from the ordered alignments, of figures 1(*b*) and 2(*b*).

The size of the particles (2.5–3.5 nm in diameter) observed in the AFM images shown in figures 1–3 is characteristic of the dimensions of MRO. The generation of linear alignments as well as the almost two-dimensional arrangement (i.e. rings) among the particles characterized by MRO gives rise to an infant surface that favours the measurement of AFM images. The immature ordered alignments among the particles characterized by MRO may thus be called supramedium-range order (SMRO). Here MRO imaged by STM (Ichikawa 1992) leads to some regular arrangement among the units as large as $\simeq$5–10 nm^2. The structural unit determined by neutron diffraction techniques is analogous to an octahedron consisting of six Te atoms around a Ge atom in the central site and is characteristic of SRO of length $\simeq$0.5 nm (see figure 8 of Ichikawa *et al* (1987)). Since the nearest-neighbour distance between the peaks in each ridge is $\simeq$0.5 nm, estimated from the STM image for the annealed $Ge_{20}Te_{80}$ glass, the regular arrangement among the ridges observed (see figure 4 of Ichikawa (1992)) should indicate MRO among Ge-centred structural units characterized by SRO. The surface, sometimes almost as large as 10 nm^2, associated with pseudo-flatness in STM images under atomic-scale resolution can be defined as the limit on the spatial extent of MRO. When we take the AFM images under nanoscopic-scale resolution, the surface of 100–300 nm^2 can be established from barely regular alignments or rings (see A or B in figures 1–3) of the particles characterized by MRO and can be interpreted in terms of a limit on the spatial extent of the SMRO.

This work was supported in part by the Suhara Memorial Fund (060 Sapporo).

References

Binnig G, Quate C F and Gerber C 1986 *Phys. Rev. Lett.* **12** 930
Elliott S R 1991 *Phys. Rev. Lett.* **67** 711
Fowler T G and Elliott S R 1987 *J. Non-Cryst. Solids* **92** 31
Ichikawa K 1992 *J. Non-Cryst. Solids* **150** 435
Ichikawa K, Kameda Y, Xu Q and Misawa M 1987 *J. Non-Cryst. Solids* **95&96** 185
Suzuki K 1987 *J. Non-Cryst. Solids* **95&96** 15
Xu Q and Ichikawa K 1986 *J. Phys. C: Solid State Phys.* **19** 7145
Yamada S and Ichikawa K 1994 unpublished work